Supporting Information

Xiuping Liu,[‡a] Yue Li,[‡b] Chunlian Hao,[b] Weidong Fan,*[b] Wei Liu,[a] Jingquan Liu[a] and Yijun Wang*[a]

[a]*School of Materials Science and Engineering, Linyi University, Linyi,*

Shandong 276000, China.

[b]*School of Materials Science and Engineering, China University of Petroleum*

(East China), Qingdao, Shandong, 266580, China.

‡ These authors contributed equally.

E-mail: wdfan@upc.edu.cn, wangyijun@lyu.edu.cn

Contents

S1. Materials and Methods

Synthesis of Ligand

The ligand 2-amino-[1,1:3,1-terphenyl]-4,4,5-tricarboxylic acid (H₃ATTCA) was prepared according to previously published procedures.[1] The detailed synthesis steps of H₃ATTCA are shown Scheme S1.
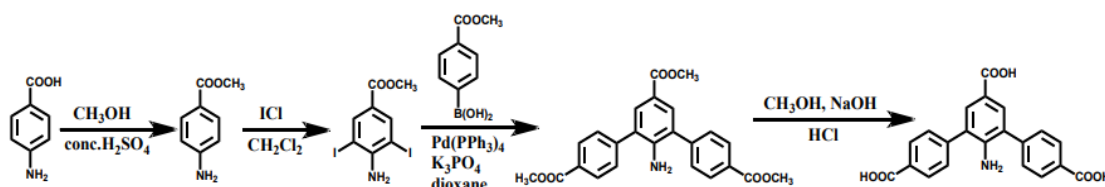
Scheme S1. Synthetic procedures of the H₃TTCA-NH₂ ligand.

(1) Methy 4-Amino Benzoate

4-Aminobenzoic acid (10 g, 0.073 mol), anhydrous methanol (125 mL), and concentrated sulfuric acid (7.5 mL) were added into a three-neck round-bottom flask. After the mixture was refluxed for 5 h by stirring, the excessive methanol was removed by air distillation. Then, the mixture was precipitated into a large amount of water and some saturated sodium carbonate solution was added. Then, the mixture was filtered and the resulting solid was collected and dried at 40 °C under vacuum for 48 h to constant weight. White sheet-shape crystal was obtained.

(2) Methyl 4-amino-3,5-diiodobenzoate

Methyl 4-aminobenzoate (3.8 g, 25 mmol) and 15 mL of CH_2Cl_2 were added to a 50 mL three-neck round bottom flask equipped with a reflux condenser and a pressure equalizing dropping funnel. The solution was placed

in an oil bath at 40 °C, and 11 mL of an ICl solution (5 M in CH_2Cl_2, 55 mmol) was added dropwise with rapid stirring over 30 min, eliciting an exothermic reaction. The resulting dark brown mixture was heated at reflux for 1.5 h. The reaction mixture was allowed to cool to room temperature, during which the product crystallized. The crystals were collected, washed with 10 mL hexanes, and dried under vacuum to afford a reddish solid. Recrystallization from methanol afforded 6.0 g (60%) of a slightly off-white solid. 1H NMR (400 MHz, $CDCl_3$) 3.88 (s, 3H), 5.06 (s, 2H), 8.32 (s, 2H). Anal. Calcd. for $C_8H_7I_2NO_2$ (mw 403): C, 23.85; N, 3.48; H, 1.75. Found: C, 23.76; N, 3.44; H, 1.71.

(3) Trimethyl 2'-amino-[1,1':3',1''-terphenyl]-4,4'',5'-tricarboxylate

Methyl 4-amino-3,5-diiodobenzoate (1.6 g, 4 mmol), Methyl 4-boronobenzoate (1.57 g, 9.6 mmol), $Pd(PPh_3)_4$ (0.15 g, 0.13 mmol) and K_3PO_4 (3.82 g, 18.0 mmol) were placed in a 500 mL two-necked round bottom flask under a N_2 gas atmosphere. The flask was further charged with a 200 mL of dry 1,4- dioxane, and the contents were heated for 48 h. After the mixture was cooled to room temperature, the solvent was removed, water was added. The water phase was washed with CH_2Cl_2. The mixed organic phases were dried with $MgSO_4$. After the solvent was removed, the crude product was purified by column chromatography with CH_2Cl_2 as the eluent. 1H NMR (400 MHz, $CDCl_3$) 3.87 (s, 3H), 3.96 (s, 6H), 7.59 (d, 4H), 7.84 (s, 2H), 8.16 (d, 4H). Anal. Calcd. for $C_{24}H_{21}NO_6$ (mw 419): C, 68.73; N, 3.34; H, 5.05. Found: C, 68.80; N, 3.29; H, 5.10.

(4) 2'-amino-[1,1':3',1"-terphenyl]-4,4",5'-tricarboxylic acid

Trimethyl 2'-amino-[1,1':3',1"-terphenyl]-4,4",5'-tricarboxylate (2.0 g, 4.8 mmol) was dissolved in 50 mL MeOH, 50 mL 2 M NaOH aqueous solution was added. The mixture was stirred at 50 °C overnight. The organic phase was removed, the aqueous phase was acidified with diluted hydrochloric acid to give yellow precipitate, which was filtered and washed with water several times. 1H NMR (400 MHz, DMSO-d_6) 5.10 (s, 2H), 7.62 (d, 6H), 8.07 (d, 4H), 12.78 (s, 3H). Anal. Calcd. for $C_{21}H_{15}NO_6$ (mw 377): C, 66.84; N, 3.71; H, 4.01. Found: C, 66.78; N, 3.73; H, 4.00.

Breakthrough experiments

The breakthrough experiments were performed on a dynamic gas breakthrough equipment. The separation of C_2H_2/C_2H_4 and C_2H_2/C_2H_6 (50/50, v/v) were carried out in a fixed bed. The column contained 626.7 mg of crystal UPC-22 for the experiment using a binary component. The flow rates (3 mL min^{-1} at 298 K and 1 atm) of gases were regulated by mass flow controllers. Before breakthrough experiments, the samples were activated at 353 K for 12 h under vacuum condition. After that, the columns were filled with a He flow. In the meantime, as a carrier gas, the He was also used to clean the system. Then, the C_2 light hydrocarbon mixture gas was stabilized by flowing through the alternative vent line for 30 min before being introduced to the column. Outlet gas from the column was monitored using gas chromatography (GC-9860-5CNJ) with the thermal conductivity detector TCD.

The absolute adsorbed amount of gas i (q_i) is calculated from the breakthrough curve by the equation:

$$q_i = \frac{F_i \times t_0 - V_{dead} - \int_0^{t_0} F_e \Delta t}{m}$$

Where F_i = influent flow rate of the specific gas (cm^3 min^{-1});

t_0 = adsorption time (min);

V_{dead} = dead volume of the system (cm^3);

F_e = effluent flow rate of the specific gas (cm^3 min^{-1});

m = mass of the sorbent (g).

The selectivity of the breakthrough experiment is defined as α = (q_1/y_1)/(q_2/y_2), where y_i is the mole fraction of gas i in the gas mixture.

Activation of UPC-22

The as-synthesized UPC-22 was washed with DMF. After fast and frequent guest solvents are exchanged for 6 h using acetone to replace the DMF and H_2O solvent molecules in the channels. After filtering, the guest-exchanged UPC-22 was activated at 80 °C for 10 h under vacuum conditions.

Synthesis of UPC-22

A mixture of $Ni(NO_3)_2 \cdot 6H_2O$ (0.10 mmol) and H_3ATTCA (0.02 mmol, H_3ATTCA =2-amino-[1,1:3,1-terphenyl]-4,4,5-tricarboxylic acid) was dissolved by dimethylformamide (DMF, 1.5 mL) and deionized water (1.5 mL) in a 10 mL glass vial, and then the sealed vial was heated to 100 °C for 72 h, which was then cooled to room temperature. The light green block crystals obtained were

washed several times with DMF for single-crystal X-ray diffraction analysis.

Yield: about 72% based on nickel.

S2. Calculation of isosteric heat of adsorption (Q_{st})

The C_2H_2, C_2H_4 and C_2H_6 adsorption isotherms measured at 273 K and 298 K were first fitted to a virial equation (eqn (1)). The fitting parameters were then used to calculate the isosteric heat of adsorption (Q_{st}) using eqn (2),

$$\ln P = \ln N + \frac{1}{T}\sum_{i=0}^{m} a_i N^i + \sum_{i=0}^{n} b_i N^i \qquad (1)$$

$$Q_{st} = -R\sum_{i=0}^{m} a_i N^i \qquad (2)$$

where P is the pressure (mmHg), N is the adsorbed quantity (mmol g^{-1}), T is the temperature (K), R is the gas constant (8.314 J K^{-1} mol^{-1}), a_i and b_i are virial coefficients, and *m* and *n* represent the number of coefficients required to adequately describe the isotherms (herein, *m*=5, and *n*=2).

S3. Calculation of selectivity via ideal adsorption solution theory (IAST)

The C_2H_2, C_2H_4 and C_2H_6 adsorption isotherms were first fitted to a dual-site Langmuir–Freundlich (DSLF) model (eqn (3)),

$$q = \frac{q_{sat,A} b_A p^{a_A}}{1 + b_A p^{a_A}} + \frac{q_{sat,B} b_B p^{a_B}}{1 + b_B p^{a_B}} \qquad (3)$$

where q is the amount of adsorbed gas (mmol g^{-1}), P is the bulk gas phase pressure (atm), q_{sat} is the saturation amount (mmol g^{-1}), *b* is the Langmuir–Freundlich parameter (atm$^{-\alpha}$), and α is the Langmuir–Freundlich exponent (dimensionless) for two adsorption sites A and B indicating the presence of weak and strong adsorption sites.

IAST starts from the Raoult's Law type of relationship between the fluid and adsorbed phase,

$$P_i = P y_i = P_i^0 x_i \qquad (4)$$

$$\sum_{i=1}^{n} x_i = \sum_{i=1}^{n} \frac{P_i}{P_i^0} = 1 \qquad (5)$$

where P_i is the partial pressure of component i (atm), P is the total pressure (atm), and y_i and x_i represent mole fractions of component i in gas and the adsorbed phase (dimensionless). P_i^0 is the equilibrium vapour pressure (atm). In IAST, P_i^0 is defined by relating to spreading pressure π,

$$\frac{\pi S}{RT} = \int_{0}^{P_i^0} \frac{q_i(P_i)}{P_i} dP_i = \Pi(constant) \qquad (6)$$

where π is the spreading pressure, S is the specific surface area of the adsorbent (m^2 g^{-1}), R is the gas constant (8.314 J K^{-1} mol^{-1}), T is the temperature (K), and $q_i(P_i)$ is the single component equilibrium obtained from isotherms (mmol g^{-1}).

For a DSLF model, we have an analytical expression for the integral,

$$\int_{0}^{P_i^0} \frac{q_i(P_i)}{P_i} dP_i = \Pi(constant) = \frac{q_{sat,A}}{\alpha_A} \ln[1 + b_A(P_i^0)^{a_A}] + \frac{q_{sat,B}}{\alpha_B} \ln[1 + b_B(P_i^0)^{a_B}] \qquad (7)$$

The isotherm parameters are derived from the previous fitting. For a binary component system the unknowns will be Π, P_1^0, and P_2^0 which can be obtained by simultaneously solving eqn (5) and (7). The adsorbed amount of each compound in a mixture is

$$q_i^{mix} = x_i q_t \qquad (8)$$

$$\frac{1}{q_T} = \sum_{i=1}^{n} \frac{x_i}{q_i(P_i^0)} \qquad (9)$$

where q_i^{mix} is the adsorbed amount of component i (mmol g^{-1}), and q_T is the total adsorbed amount (mmol g^{-1}).

The adsorption selectivities S_{ads} were calculated using eqn (10).

$$S_{ads} = \frac{q_1/q_2}{p_1/p_2} \ (10)$$

In this study, IAST calculations were carried out assuming a C_2H_2/C_2H_4 and C_2H_2/C_2H_6 binary mixed gas with a molar ratio of 50:50, 1:99 at 273 K and 298 K and pressures up to 1 atm.

S4. Crystal data of complex UPC-22

Table S1. Crystal data and structure refinement for complex UPC-22

Parameters of crystal structure	Values
Formula	$C_{21}Ni_3O_{12}NH_{24}$
M	659
Crystal system	orthorhombic
Space group	*I2b2*
a/Å	34.854(2)
b/Å	26.440(2)
c/Å	6.3950(3)
α/deg	90.0
β/deg	90.0
γ/deg	90.0
V/Å³	5893.2(6)
Z	4
GOF	1.006
$R_1{}^a$/$wR_2{}^b$ I > 2σ(I)	0.1823, 0.5173

R_1, wR_2 (all data)	0.1940, 0.5266
R_{int}	0.0161

$^aR_1 = \Sigma||F_o| - |F_c||/\Sigma|F_o|$. $^bwR_2 = [\Sigma w(F_o^2 - F_c^2)^2/\Sigma w(F_o^2)^2]^{0.5}$.

S5. Determination of single-crystal structure

Single crystal of the prepared complex with appropriate dimensions was chosen under an optical microscope and quickly coated with high vacuum grease (Dow Corning Corporation) before being mounted on a glass fiber for data collection. Data for UPC-22 were collected on Super Nova diffractometer equipped with a Cu-K_α radiation X-ray sources (λ = 1.54 Å) and an Eos CCD detector under 100 K. For UPC-22, data were measured using scans of 0.5° per frame for 10 s until a complete hemisphere had been collected. Data reduction was performed with the CrysAlisPro package, and an analytical absorption correction was performed. The structures were treated anisotropically, whereas the aromatic and hydroxy-hydrogen atoms were placed in calculated ideal positions and refined as riding on their respective carbon or oxygen atoms. Structure was examined using the Addsym subroutine of PLATON[2] to assure that no additional symmetry could be applied to the model.

S6. Computational methods

Grand canonical Monte Carlo (GCMC) calculations:

In this work, the adsorption of pure C_2H_2, C_2H_4 and C_2H_6 adsorption in UPC-22 was simulated using the grand canonical Monte Carlo (GCMC) method implemented in the Material Studio 8.0. Periodic boundary conditions were applied in three dimensions. A combination of site−site Lennard–Jones (LJ) and Coulombic potentials was used to calculate the gas-gas and gas−framework interactions. The site−site LJ potential was described by the LJ (12, 6) model, and the electrostatic interaction was calculated via the Coulomb law. All the interaction parameters conform to Lorentz−Berthelot mixing rules, i.e., $\varepsilon_{ij} = (\varepsilon_{ii}\varepsilon_{jj})^{1/2}$, $\sigma_{ij} = (\sigma_{ii} + \sigma_{jj})/2$.[3] During the simulations, the framework was rigid considering the negligible influence of framework flexibility on the adsorption of gas under the low-energy conditions.[4] Atomic partial charges derived from Q_{Eq} method. All parameters for the atoms were modeled with the universal forcefield (UFF) embedded in the MS modeling package. The cutoff distance for truncation of the intermolecular (LJ) interactions was set to 8 Å, and the Ewald

sum technique was used to compute the electrostatic interaction. The number of trial moves was 2×10^7. The first 10^7 moves were used for equilibration, and the subsequent 10^7 moves were performed to sample the desired properties.

Density functional theory (DFT) calculations:

DFT calculations were performed to provide the atomic partial charges on the UPC-22 framework for the grand canonical Monte Carlo (GCMC) calculations as well as to give the optimized structures and energies of CH_4 interaction with the fragmented cluster of UPC-22. We used the Perdew−Burke−Ernzerhof (PBE) functional under the generalized gradient approximation (GGA) functional with the double-ξ numerical polarization (DNP) basis set implemented in the DMol^3 program package in the Materials Studio of Accelrys Inc for our calculations. Since calculations using the whole unit cells are too expensive, we used fragmented cluster models cleaved from the unit cells for modeling the partial charges, structures, and energies, the cleaved bonds at the boundaries of the clusters were saturated with protons (hydrogens) (see Fig. 5, S10-S11). The tolerances of energy, gradient and displacement convergence were 1×10^{-5} hartree, 2×10^{-3} hartree Å^{-1}, and 5×10^{-3} Å, respectively. The atomic charges in complex UPC-22 were estimated by fitting to the electrostatic potential (ESP) obtained with the CHELPG method,[5] which has been successfully used to describe the behavior of other MOFs.[6] The adsorption energies (ΔE_{ad}) of gas molecules with the fragmented cluster were calculated by $\Delta E_{ad} = E_{gas-cluster} - E_{gas} - E_{cluster}$, where E_{gas}, $E_{cluster}$, and $E_{gas-cluster}$

are the total energies of the gas molecule, the fragmented cluster, and the adsorption system at their optimized geometries, respectively.
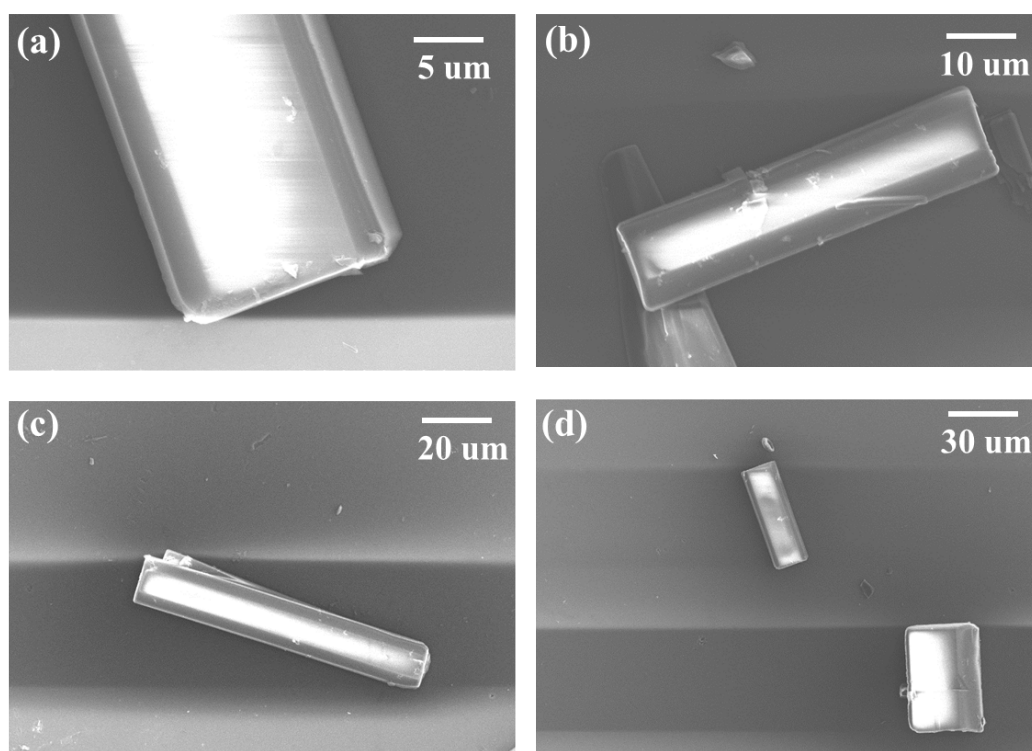
S7. SEM images of UPC-22

Fig. S1 SEM images of porous UPC-22.

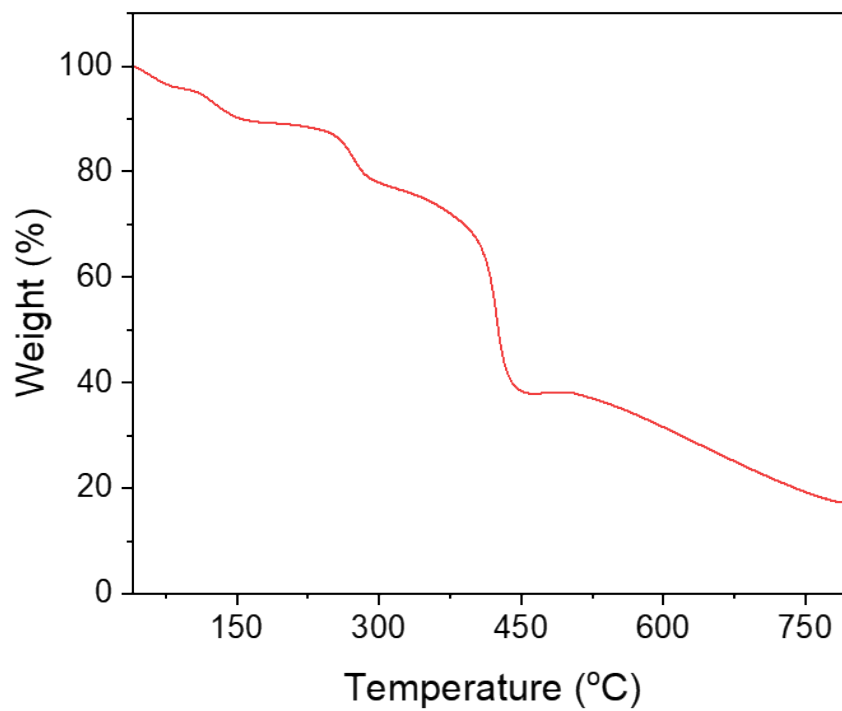## S8. The TGA curve of UPC-22

Fig. S2 TGA curve of UPC-22.
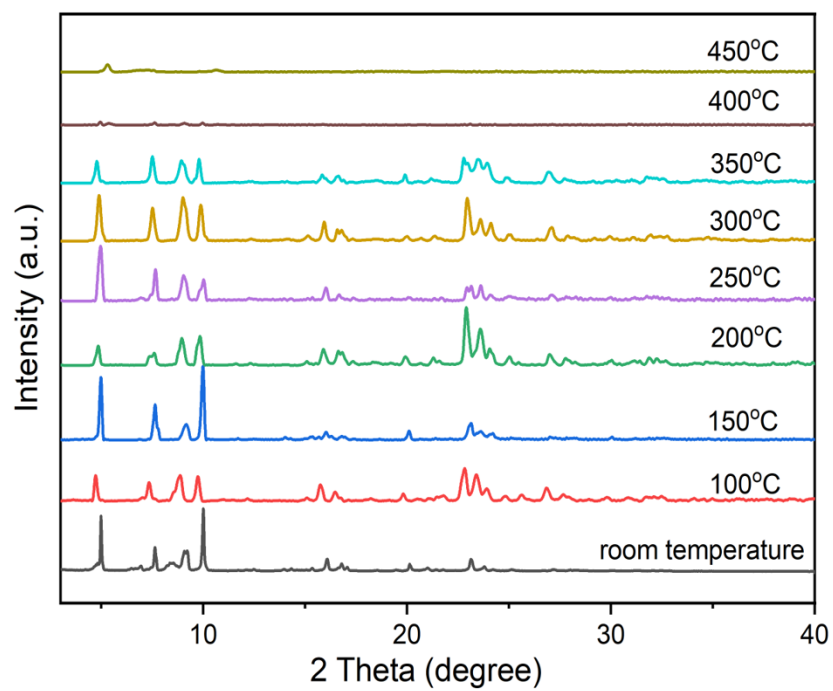
S9. The PXRD curve of UPC-22

Fig. S3 The PXRD patterns of UPC-22 at variable temperature.
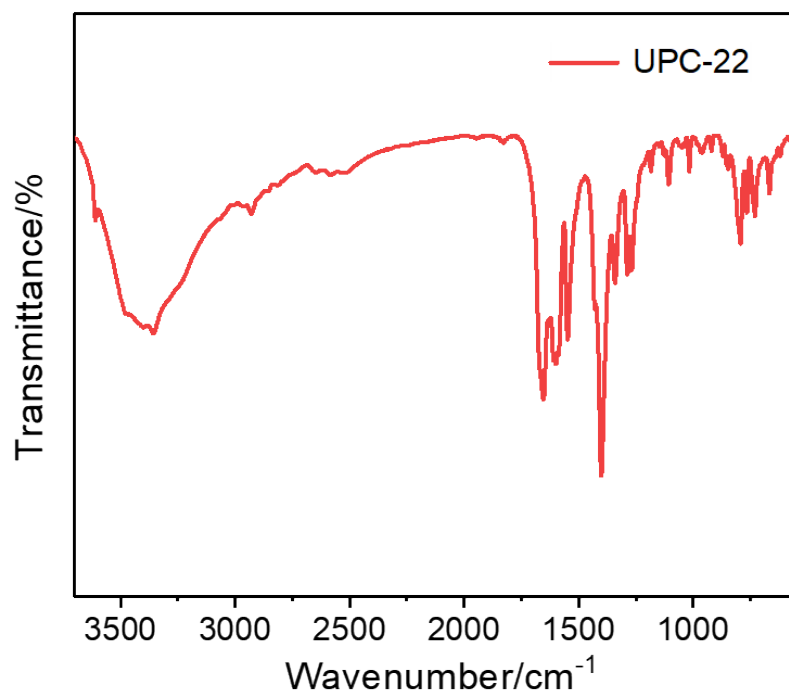
S10. The IR curve of UPC-22

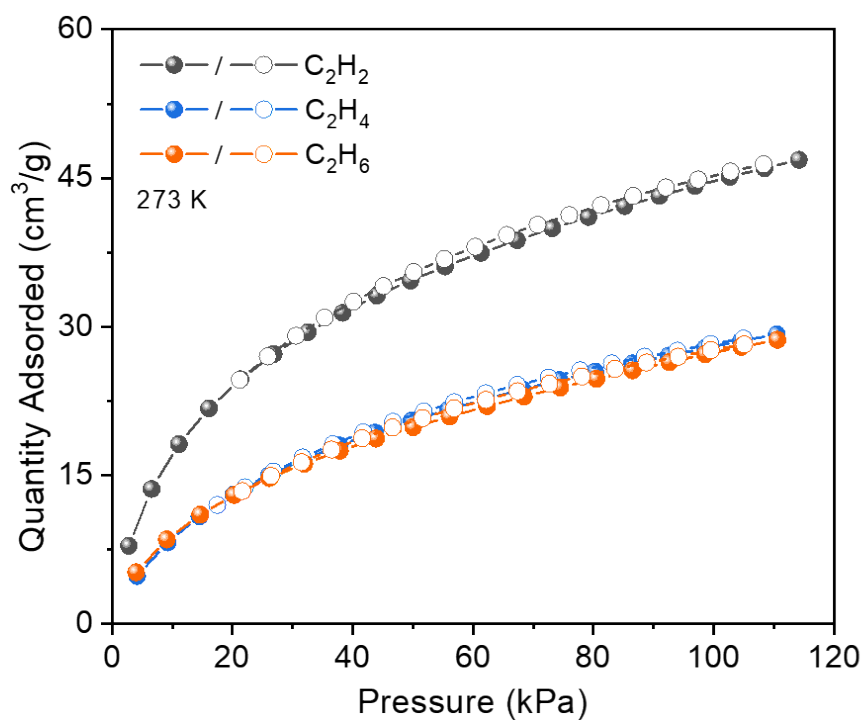**Fig. S4** IR curve of UPC-22.

S11. The adsorption and separation properties of UPC-22

Fig. S5 The C_2H_2, C_2H_4, C_2H_6 adsorption isotherms of UPC-22 at 273 K.
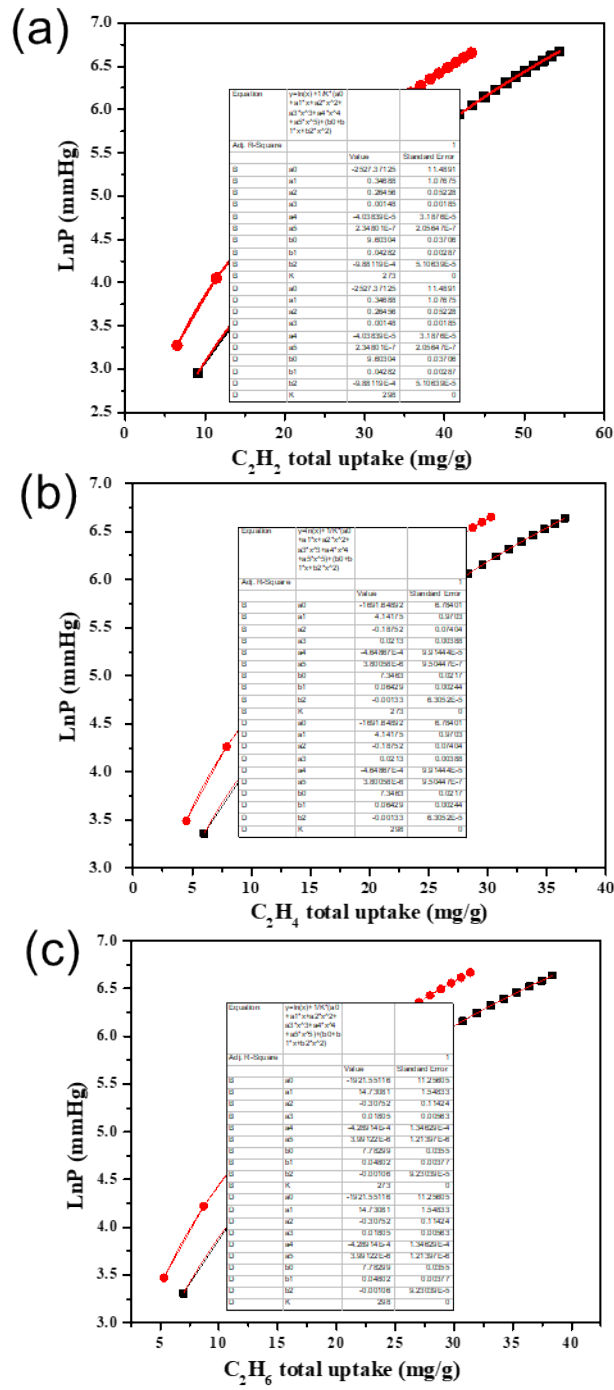
Fig. S6 Derivation of Q_{st} for C_2H_2, C_2H_4, and C_2H_6 adsorption of UPC-22 from virial fitting of the total adsorption isotherm data. The virial coefficients are shown on the right.
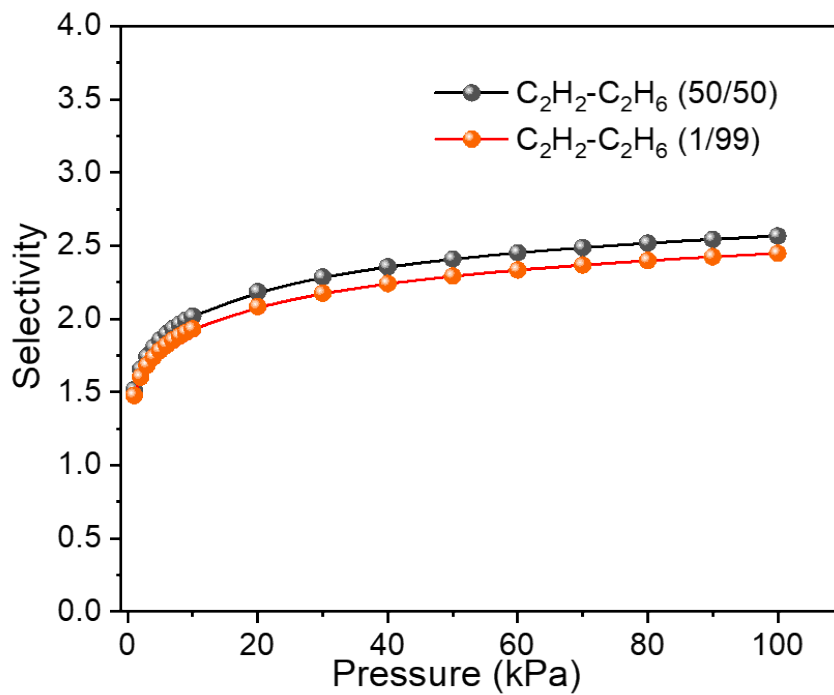
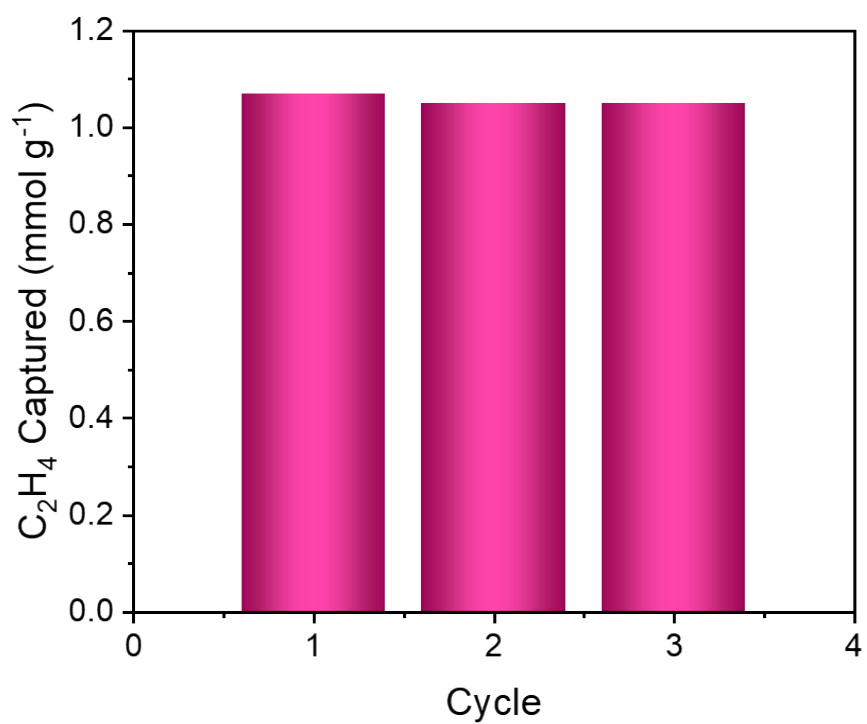**Fig. S7** Adsorption selectivities of UPC-22 calculated by the IAST method for mixtures of C_2H_2/C_2H_6 at 298 K.

Fig. S8 Separation cycling test of equimolar C_2H_2/C_2H_4 mixtures in an absorber bed packed with UPC-22 at 298 K and 1 bar.
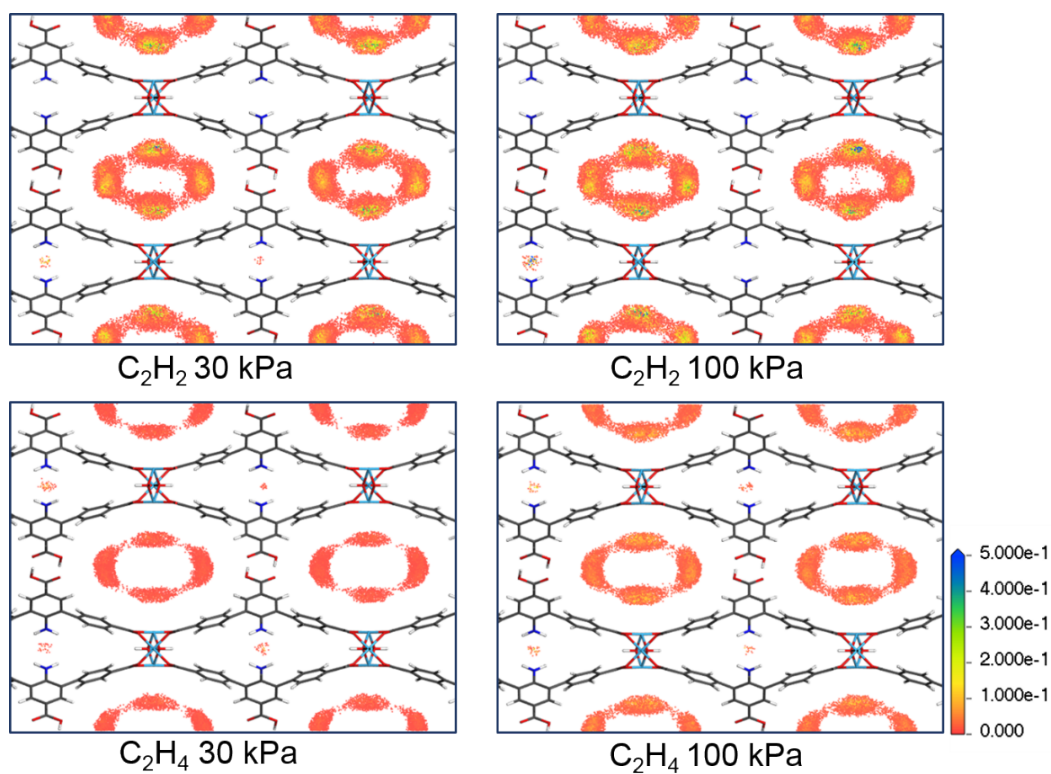
S12. The GCMC and DFT calculations for UPC-22

C$_2$H$_2$ 30 kPa

C$_2$H$_2$ 100 kPa

C$_2$H$_4$ 30 kPa

C$_2$H$_4$ 100 kPa

5.000e-1
4.000e-1
3.000e-1
2.000e-1
1.000e-1
0.000

Fig. S9 Density distribution of the center-of-mass of C$_2$H$_2$ and C$_2$H$_4$ molecules in the unit cell of UPC-22 at 298 K and different pressures (30 and 100 kPa) simulated by GCMC.
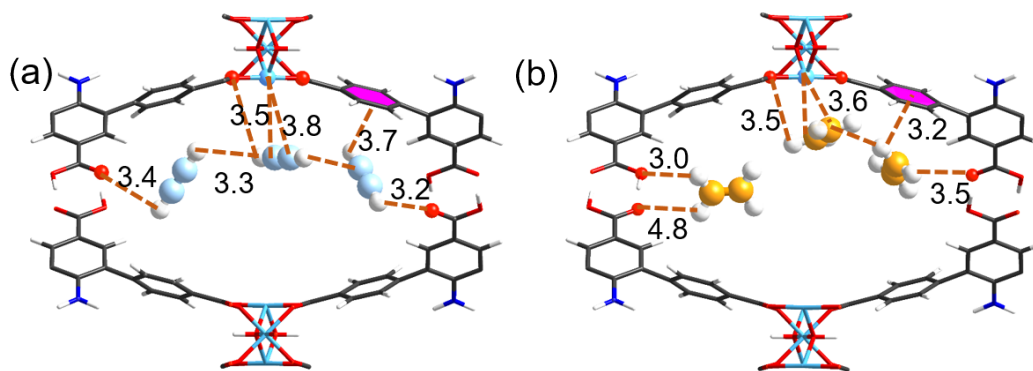
Fig. S10 Results of the GCMC simulations showing preferential binding sites between the adsorbed molecule and UPC-22: (a) C_2H_2 and (b) C_2H_4.
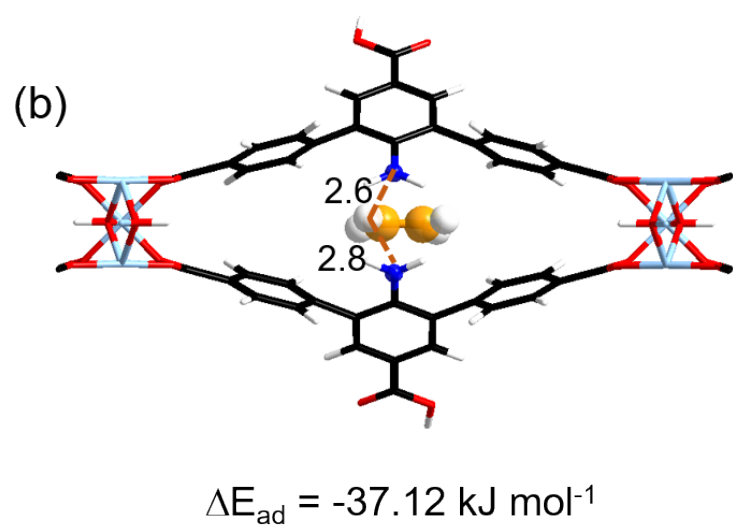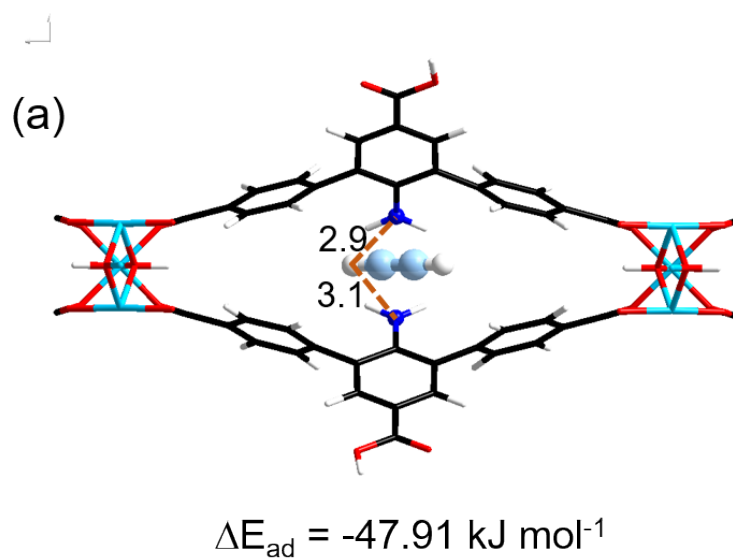
(a)

ΔE_{ad} = -47.91 kJ mol^{-1}

(b)

ΔE_{ad} = -37.12 kJ mol^{-1}

Fig. S11 Binding sites of C_2H_2 and C_2H_4 in UPC-22 determined by DFT simulations (a) and (b).

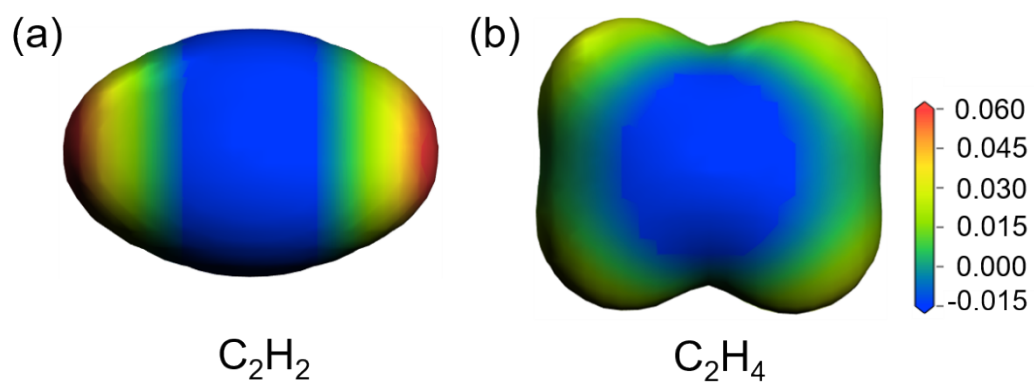**Fig. S12** Electrostatic potential (ESP) of C_2H_2 and C_2H_4 mapped onto the 0.05 e $Å^{-3}$ electron density isosurfaces.

References

1. W. Fan, H. Lin, X. Yuan, F. Dai, Z. Xiao, L. Zhang, L. Luo and R. Wang, Expanded Porous Metal–Organic Frameworks by SCSC: Organic Building Units Modifying and Enhanced Gas-Adsorption Properties. Inorg. Chem., 2016, 55, 6420–6425.

2. S. Ding, X. Sun, Y. Zhu, Q. Chen, Y. Xu, Europium(III) sulfate hydroxide, *Crystallogr,* 2006, **62**, i269–i271.

3. A. A. Clifford, P. Gray, N. Platts, Lennard-Jones 12: 6 parameters for ten small molecules, *J. Am. Chem. Soc.,* 1977, **73**, 381−382.

4. Q. Yang, D. Liu, C. Zhong, R. J. Li, Development of computational methodologies for metal–organic frameworks and their application in gas separations, *Chem. Rev.,* 2013, **113**, 8261−8323.

5. U. C. Singh, A. P. Kollman, An approach to computing electrostatic charges for molecules, *J. Comput. Chem.,* 1984, **5**, 129–145.

6. R. Babarao, J. Jiang, Upgrade of natural gas in rhozeolite-like metal–organic framework and effect of water: a computational study, *Energy Environ. Sci.,* 2009, **2**, 1088–1093.